Mesoscopic supersolid of dipoles in a trap

A. E. Golomedov,[1] G. E. Astrakharchik,[2] and Yu. E. Lozovik[1,3]
[1]*Institute of Spectroscopy, 142190 Troitsk, Moscow Region, Russia*
[2]*Departament de Física i Enginyeria Nuclear, Campus Nord B4-B5, Universitat Politècnica de Catalunya, E-08034 Barcelona, Spain*
[3]*Moscow Institute of Physics and Technology (State University), Dolgoprudny, Moscow Region, Russia*
(Received 20 May 2011; published 14 September 2011)

A mesoscopic system of dipolar bosons trapped by a harmonic potential is considered. The system has a number of physical realizations including dipole excitons, atoms with large dipolar moment, polar molecules, and Rydberg atoms in inhomogeneous electric field. We carry out a diffusion Monte Carlo simulation to define the quantum properties of a two-dimensional system of trapped dipoles at zero temperature. In dimensionless units the system is described by two control parameters, namely, the number of particles and the strength of the interparticle interaction. We have shown that when the interparticle interaction is strong enough a mesoscopic crystal is formed. As the strength of interactions is decreased a multistage melting takes place. Off-diagonal order in the system is tested using natural-orbitals analysis. We have found that the system might be Bose condensed even in the case of strong interparticle interactions. There is a set of parameters for which a spatially ordered structure is formed while simultaneously the fraction of Bose-condensed particles is nonzero. This might be considered as a realization of a mesoscopic supersolid.

DOI: 10.1103/PhysRevA.84.033615 PACS number(s): 03.75.Hh, 05.30.Fk, 67.80.K−

I. INTRODUCTION

Bose-Einstein condensation (BEC) is a phenomenon that has been attracting great attention since its prediction in 1924 [1,2]. Theoretical description of condensate properties is commonly based on the mean-field Gross-Pitaevskii equation [3] which applies to a dilute Bose gas. This assumption is not fulfilled in systems with strong correlations.

This is the case of a two-dimensional rather dense dipole system of indirect excitons in coupled quantum wells or in a single quantum well in strong electric field [4]. At densities much smaller than a^{-2} (with a being the characteristic exciton size) exchange effects are greatly suppressed by the dipole-dipole repulsion, so dipole excitons can be treated as Bose particles. The exciton confinement can be created by inhomogeneous electric field or inhomogeneous deformation of semiconductors. The inhomogeneous electric field can be generated, for example, by a tip a of scanning probe microscope or by a profiled controlling gate (see [5] and references therein).

The dipolar interactions are also important in atomic gases with a large dipolar moment. The Bose-Einstein condensation has been achieved in ^{52}Cr atoms possessing a large permanent dipolar moment [6]. In this system there is a competition between short-range interactions and long-range dipolar forces. Strong dipolar effects have been experimentally observed in trapped chromium atoms; see Refs. [7–10]. A large dipolar moment can be induced in polar molecules by applying an external electric field. Recently the quantum regime of ^{40}K^{87}Rb fermionic polar molecules has been reached and dipolar collisions in such systems has been experimentally studied [11,12]. A Rydberg atom (an atom with one electron excited to a very high principal quantum number [13]) has a very large size and a very large polarizability; i.e., a large dipole moment can be inducted in moderate electric field. An electric field aligns dipolar moments so that the interaction in a 2D system has a dipolar $1/r^3$ form. An optical trapping can be used to confine the system of Rydberg atoms [14].

A close relation between two quantum phenomena, BEC and superfluidity, suggests that a system might be superfluid if a part of it is Bose condensed. Moreover, at the same time the system can possess a crystal order, i.e., can be a supersolid. A finite superfluid signal was reported in a number of recent experiments with cold helium in solids (see [15–22]). It is probable that the superfluid signal observed in experiments is due to the presence of defects. We note that mesoscopic trapped systems are good candidates for being supersolids as no perfect commensurate crystalline structure can be formed and defects are intrinsically present in the system. We perform numerical simulations of a trapped system of excitons with dipolar interaction, to obtain structure properties and to study how the crystal-like order is formed in the system.

In the regime when dipole-dipole repulsions are weak, analytical approaches based on the mean-field approximation provide a good description of the system, but fail when the density is large. Instead Monte Carlo methods have no such limitations and can be successfully applied to strongly interacting systems. In Ref. [23] properties of a classical dipolar system in a harmonic trap at low finite temperature were studied. Path-integral Monte Carlo (PIMC) simulation of trapped clusters was performed in works by Lozovik *et al.* [24] and Pupillo *et al.* [14] for dipolar interaction, and for Coulomb interaction by Filinov *et al.* [25]. The PIMC technique is useful for simulation of the properties of quantum systems at a finite temperature, while the smaller the temperature is, the more difficult it is to obtain accurate results, which makes the simulation of the ground state of the system extremely difficult. Instead, the diffusion Monte Carlo method is well suited for studying ground-state properties. In references [26–29] two-dimensional (2D) systems of dipoles in the absence of an external potential were studied. It was shown that at large density a crystal is formed. Nonzero superfluid and condensate fractions have been found in finite-size crystals and in crystals with vacancies.

In the present work we study the effects of a harmonic confinement in a 2D geometry. Our motivation for expecting

a coexistence of a finite condensate fraction and broken rotational symmetry (i.e., "supersolidity") in trapped systems is twofold: (i) Small trapped systems are mesoscopic, and (ii) inherent incommensurability between the spherical geometry of the trap and the triangular geometry of a 2D triangular lattice leads to an effective introduction of defects in the lattice, which might lead to the appearance of superfluidity. To the best of our knowledge quantum systems of two-dimensional trapped dipoles at zero temperature so far were not well studied.

This work is organized as follows. In Sec. II we outline the model Hamiltonian and describe the methods used in the simulation. In Sec. III we describe the method of natural orbitals used for studying coherence in the system; in this section we generalize the method used in 3D systems (see [30,31]) to the case of 2D. In Sec. IV we present the obtained results, and in Sec. V we draw conclusions.

II. MODEL SYSTEM AND NUMERICAL APPROACH

We consider a two-dimensional system of N dipolar bosons in a harmonic trap with frequency ω. Such a system is described by the Hamiltonian

$$\hat{H} = \sum_{i}^{N} -\frac{\hbar^2}{2m}\nabla_i^2 + \sum_{i}^{N}\frac{1}{2}m\omega^2 r_i^2 + \sum_{i<j}^{N}\frac{d_{\rm dip}^2}{r_{ij}^3}. \qquad (1)$$

The second term in the Hamiltonian (1) is associated with harmonic confinement potential, the third term describes the dipolar interaction between particles, m is the mass of a particle, and $d_{\rm dip}$ is its dipole moment. It is convenient to use oscillator units in the problem, that is, to measure length in units of oscillator length $a_0 = \sqrt{\hbar/m\omega}$ and energy in units of $\hbar\omega$. The dimensionless Hamiltonian is then

$$\hat{H} = \frac{1}{2}\sum_{i}^{N}\left(-\nabla_i^2 + r_i^2\right) + \sum_{i<j}^{N}\frac{d}{r_{ij}^3}, \qquad (2)$$

where $d = d_{\rm dip}^2/a_0^3\hbar\omega$ is a dimensionless coupling parameter, which can be interpreted as the ratio of the typical energy of the dipolar interaction energy $E_{\rm int} = d_{\rm dip}^2/a_0^3$ and the characteristic energy of a harmonic oscillator confinement $E_{\rm trap} = \hbar\omega$.

In order to study system properties we use Monte Carlo (MC) methods. A number of MC methods may be employed for simulation of quantum systems: variational Monte Carlo (VMC), diffusion Monte Carlo (DMC), path-integral Monte Carlo (PIMC), path-integral ground state, etc. In the present work we are interested in ground-state (zero temperature) properties and we investigate them by means of VMC and DMC techniques.

In the VMC method one samples particle distribution according to a chosen trial wave function. By doing that it is possible to obtain mean values of an observable by averaging its value over the chain of realizations of particles coordinates. The method proposed by Metropolis *et al.* [32] is used to generate such a chain.

Although we do not know the many-body wave function exactly, a physically sound ansatz may be used for the trial wave function so that it depends on particle coordinates and a set of additional parameters. Those parameters, referred to as variational parameters, are used to minimize energy corresponding to this wave function. A variational principle applies; that is, the variational energy calculated in this way is always larger than the ground-state energy and equal to it when the trial wave function coincides with the ground-state wave function.

The main idea of the DMC technique is to solve the Schrödinger equation in the imaginary time. For sufficiently long evolution of an arbitrary wave function in the imaginary time its projection to the excited states is exponentially suppressed compared to its projection to the ground state. The problem is that one would rather prefer to sample the square of the absolute value of the wave function (probability density) than the wave function itself, because average values of an observable with diagonal operator is defined as an integral where the observable is integrated with weight equal to the absolute value of the wave function squared. But it is impossible to introduce a closed real-valued equation defining the time evolution of the probability density. A common choice is to calculate mixed estimators for observables where the observable is integrated with weight equal to $f(\mathbf{R},t) = \psi_T(\mathbf{R})\psi_0(\mathbf{R},t)$, with $\psi_T(\mathbf{R})$ being the trial wave function and $\psi_0(\mathbf{R},t)$ the ground-state wave function. A mixed estimator introduces some bias due to a particular choice of the trial wave function, unless the observable commutes with the Hamiltonian. An important example of a mixed estimator being exact is in the evaluation of the ground-state energy.

For other observables one can reduce this bias by extrapolating the mixed estimator to the exact one,

$$A_{extr} = 2A_{\rm mixed} - A_{\rm trial}. \qquad (3)$$

Here $A_{\rm mixed} = \int \psi_T A \psi_0$ is the mixed estimator of an observable A and $A_{\rm trial} = \int \psi_T^* A \psi_T$ is a variational estimator. This extrapolation is accurate to the second order of difference between the trial wave function and the exact one. We applied the extrapolation for all observables that do not commute with the Hamiltonian.

To reduce the extrapolation error it is important that the projection of the trial wave function to the ground state is as large as possible. We construct the trial wave function in the Nosanow-Jastrow form

$$\Psi_T(\mathbf{R}) = \prod_{i}^{N} f(r_i)\prod_{i<j}^{N} g(r_{ij}), \qquad (4)$$

where $\mathbf{R} = \{r_1, r_2, \ldots, r_N\}$ stands for a point in $2N$-dimensional phase space, and $f(r)$ and $g(r)$ are one- and two-body correlation terms. The first term in $\Psi_T(\mathbf{R})$ takes into account one-body physics and describes the effects of the harmonic oscillator, while the second term introduces interparticle correlations. For different values of the interaction strength d we have used several forms of $f(r)$ and $g(r)$.

A. Gas of dipoles

An exact expression for the one-body terms $f(r_i)$ of the wave function (4) is known in the limit of an ideal Bose gas $d \to 0$ and is given by Gaussians $f_{ho}(r_i) = \exp(-r_i^2/2a_0^2)$.

We keep this functional dependence form for finite values of the interaction strength d:

$$f(r) = \exp(-\alpha r^2), \tag{5}$$

with a single variational parameter α, which value is fixed by minimizing the variational energy.

The long-distance physics are dominated by the Gaussian dependence in $f(r)$, so the main requirement for the two-body Jastrow term is to describe correctly short-range physics. When two particles come close to each other the influence of other particles can be neglected and the two-body Jastrow term in the trial wave function (4) can be well approximated by the zero-energy scattering solution of the two-body problem [27],

$$g(r) = K_0(2\sqrt{d/r}). \tag{6}$$

The resulting trial wave function is

$$\psi(\mathbf{R}) = \prod_i^N \exp\left(-\alpha r_i^2\right) \prod_{i\neq j}^N K_0(2\sqrt{d/r_{ij}}). \tag{7}$$

This wave function preserves rotational symmetry and is a trap analog of the wave function of a homogeneous gas.

B. Crystal of dipoles

When a crystal is formed the system loses the translational symmetry. To take this into account one has to use a proper symmetry in the trial wave function. We introduce a localizing "crystal" term in the trial wave function (TWF),

$$u(\mathbf{R}) = \prod_j^{N_c} \sum_i^N \exp\left[-\beta\left(\mathbf{r}_i - \mathbf{r}_j^c\right)^2\right], \tag{8}$$

where β is a variational parameter. Each Gaussian term describes particle localization close to sites r_j^c, the total number of sites in the crystal being denoted by N_c. We have used the classical Monte Carlo method combined with gradient descent optimization to obtain the position of sites $\mathbf{r}_j^c$ for a given particle number N_c. In a quantum system the zero-point fluctuations effectively delocalize particle positions; this increases the potential energy due to dipolar repulsion. In order to diminish the effect of the interparticle repulsion the system size increases. We take this effect into account by scaling the classical positions as $\mathbf{r}_j^c \to \gamma \mathbf{r}_j^c$ with the factor γ optimized by minimizing the energy in variational Monte Carlo calculations.

Combining Eq. (8) with the trial wave function of gas Eq. (7) we obtain the final expression for the crystal trial wave function:

$$\psi(\mathbf{R}) = \left[\prod_i^N \exp\left(-\alpha r_i^2\right) \prod_{i\neq j}^N K_0(2\sqrt{d/r_{ij}})\right] \times \prod_j^{N_c} \sum_i^N \exp\left[-\beta\left(\mathbf{r}_i - \mathbf{r}_j^c\right)^2\right]. \tag{9}$$

Such a wave function breaks the rotational symmetry and is analogous to the crystal wave function in the absence of a trap, where the particles are localized close to lattice sites.

The typical dependence of the variational energy on parameter β is shown in Fig. 1. There are two minima. The first one at $\beta = 0$ corresponds to a delocalized system or a gas state. The second minimum is located at $\beta \neq 0$ and corresponds to a localized system or a crystal.

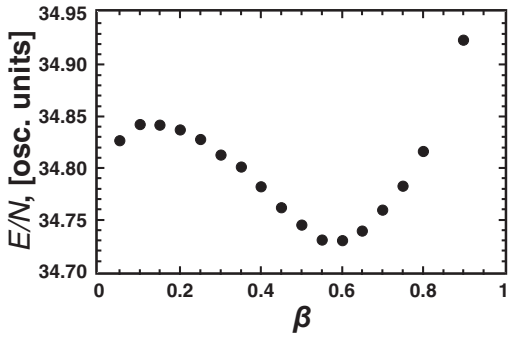

FIG. 1. Variational energy as a function of the variational parameter β in a cluster of $N = 32$ particles with interaction strength $d = 100$.

C. Gas of strongly correlated dipoles

Crystal and gas wave functions provide a good description in corresponding limits, but their use for intermediate values of the interaction strength produces a large error in mixed estimators. The smaller the difference between the trial and ground state and wave functions is, the smaller is the error. To reduce this difference in the region of intermediate interaction strength, we introduce a shell term in the trial wave function,

$$s(r) = \left[\sum_{i=1}^{N_p} a_i \exp\left[-\left(r - r_i^s\right)^2/\sigma_i^2\right]\right]^\gamma, \tag{10}$$

where r_i^s is the separation of the ith shell from the center of trap, σ_i is the width of the ith shell and a_i is its amplitude, and γ is a variational parameter. The parameters of the shells are optimized so that $s(r)$ (for $\gamma = 1$) is the best approximation of the ratio of variational and diffusion radial distributions. The variational result for the radial distribution calculated with $s(r)$ reproduces closely the DMC mixed estimator calculated by using the "gas wave function," Eq. (7), and it means that the trial wave function is better when the shell term $s(r)$ is used. The resulting trial wave function for this case is

$$\psi(\mathbf{R}) = \prod_i^N \left(\exp\left(-\alpha r_i^2\right)\left[\sum_{i=1}^{N_p} a_i \exp\left[-\left(r - r_i^s\right)^2/\sigma_i^2\right]\right]^\gamma\right) \times \prod_{i\neq j}^N K_0(2\sqrt{d/r}). \tag{11}$$

This trial wave function does not break the rotation symmetry while it supports radial ordering of the particles (i.e., formation of shells). Similar symmetries were encountered in a multistage melting of trapped clusters where at intermediate temperatures the shells start to rotate and are "orientationally disordered" [23,33].

III. BOSE-EINSTEIN CONDENSATE

To test the coherence in the system and to calculate the condensate fraction we study the spectral properties of the one-body density matrix (OBDM). The OBDM is defined as

$$\rho(\mathbf{r},\mathbf{r}') = \langle\hat{\Psi}^{\dagger}(\mathbf{r}')\hat{\Psi}(\mathbf{r})\rangle, \tag{12}$$

where $\hat{\Psi}(\mathbf{r})$ is the field operator that annihilates a particle at the point $\mathbf{r}$. Using single-particle states $\phi_i(\mathbf{r})$, we expand the field operator,

$$\hat{\Psi}(\mathbf{r}) = \sum_i \phi_i(\mathbf{r})\hat{a}_i, \tag{13}$$

where $\hat{a}_i$ is the bosonic annihilation operator that annihilates a particle in the state $|i\rangle$. Substituting (13) into (12) one obtains the spectral decomposition

$$\rho(\mathbf{r},\mathbf{r}') = \sum_{ij} \phi_i^*(\mathbf{r})\phi_j(\mathbf{r}')N_i\delta_{ij}. \tag{14}$$

The OBDM is diagonal in the single-particle state basis, and natural orbitals $\phi_i(\mathbf{r})$ (occupation numbers N_i) are its eigenvectors (eigenvalues). The condensate is described by the orbital $\phi_0(\mathbf{r})$ with the macroscopic occupation number, and the condensate fraction is $n_0 = N_0/N$.

In two dimensions the OBDM is a function of four arguments, and eigenfunctions $\phi(\mathbf{r})$ are functions of two arguments. The problem for the eigenvalues can be simplified if there is a cylindrical symmetry of the problem. In this case the OBDM depends on angle $\theta = \phi - \phi'$ between vectors $\mathbf{r}$ and $\mathbf{r}'$, rather than on two angles ϕ and ϕ'. Furthermore OBDM can be expanded in a series of angular momentum components:

$$\rho(\mathbf{r},\mathbf{r}') = \frac{1}{\sqrt{2\pi}} \sum_l \rho_l(r,r') \exp(il\theta) \tag{15}$$

with the projection of the OBDM to the state with angular momentum l, $l = 0, \pm 1 \ldots$ given by

$$\rho_l(r,r') = \int d\theta dr_2 \ldots dr_N \Psi^*(r,r_2,\ldots,r_N) \times \exp(-il\theta)\Psi(r,r_2,\ldots,r_N). \tag{16}$$

Further, the one-body orbitals can be expanded in terms of the angular momentum

$$\begin{aligned} \phi_k(\mathbf{r}) &= R_{nl}(r)\Phi_l(\varphi), \\ \Phi_l(\varphi) &= \frac{1}{\sqrt{2\pi}} \exp(il\varphi), \end{aligned} \tag{17}$$

where compound index k consists of two indexes l,n. Substituting Eq. (17) into Eq. (14) we obtain the representation of the lth OBDM in terms of natural orbitals,

$$\rho_l(r,r') = \sum_i \phi_{il}^*(r)\phi_{il}(r')N_{il}. \tag{18}$$

Matrices $\rho_l(r,r')$ can be sampled in a Monte Carlo simulation according to Eq. (16) and are "usual" algebraic matrices understood as functions of two scalar arguments, which can be readily diagonalized using standard matrix methods. For condensate study we consider only components with angular moment $l = 0$. To solve this equation numerically we introduce regularized functions

$$u_{il}(r) = \phi_{il}(r)\sqrt{r}. \tag{19}$$

These functions $u_{il}(r)$ are better than $\phi_{il}(r)$ in calculations, because they are well behaved near $r = 0$. In terms of u_{il}(r), the relation Eq. (18) reads as

$$\sqrt{r}\rho_l(r,r')\sqrt{r'} = \sum_i u_{il}^*(r)u_{il}(r')N_{il}. \tag{20}$$

We solve this equation and obtain the condensate wave function

$$\phi_0(r) = u_{00}(r)/\sqrt{r}. \tag{21}$$

IV. RESULTS

In this section we present the results of DMC and VMC simulations of the system. In the first part of the section we discuss structural properties of the system and in the second part we study properties of the condensate.

A. Structural properties

We perform a Monte Carlo study of structural and energetic properties of dipolar clusters by doing calculations with different trial wave functions. We have tested the quality of different trial wave functions for a cluster of $N = 32$ particles in the strongly interacting regime $d = 200$. The results obtained for the energy are summarized in Table I.

One can see that the best variational energy of the cluster with strong interactions $d = 200$ is the one obtained using the crystal trial wave function (8). The energy of a crystal in the DMC calculation is larger than both the DMC energy of a gas and the DMC energy of a strongly correlated gas with formed shells. The best DMC energy of the system is given by the wave function shell structured gas (11).

DMC calculations of the energy of the cluster with different interaction strengths showed that the gas phase is energetically preferable for values of interaction strength smaller than ~100; in the region of $100 \lesssim d \lesssim 400$ strong correlated gas is energetically preferable and for values of d larger than ~400 a full crystal is formed. Figure 2 shows the radial distribution of particles $R(r)$ for different values of d obtained with a gas trial wave function. One finds that $R(r)$ becomes nonmonotonic as the interaction increases and

TABLE I. Ground-state energy per particle for $N = 32$ particles for $d = 200$; energy is measured in units of $\hbar\omega$. Number in parentheses shows the error on the last digit.

Method and Trial Wave Function	Energy per Particle
VMC, gas TWF	44.9584(9)
DMC, gas TWF	44.4201(6)
VMC, crystal TWF	44.848(1)
DMC, crystal TWF	44.4491(5)
VMC, TWF with shell term	44.8523(7)
DMC, TWF with shell term	44.4145(8)

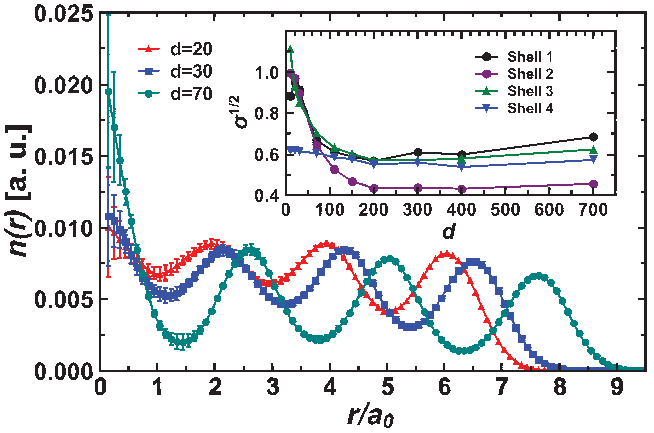

FIG. 2. (Color online) Radial distribution (main plot) and width of the shells (inset) for different values of interaction strength d in a system of $N = 32$ particles. All distribution profiles are normalized to the total number of particles; i.e., $\int n(r)2\pi r\, dr = N$.

a shell structure is formed. We find that the shells can be well approximated by a set of Gaussians. The width of the Gaussians (see inset in Fig. 2) saturates to a constant value when d is large enough. This fact can be explained if we assume that dipoles are moving around crystal sites in the mean field associated with other particles and consider a generalized interaction law $1/r^{\alpha}$, where $\alpha > 1$. In a homogeneous crystal the first nondisappearing term of the mean field is a quadratic one with frequency $\omega_{mf} \sim V''_{\text{real}}(r)|_{r=r_0} = \alpha(\alpha-1)V(r_0)/r_0^2$, where r_0 is the mean interparticle distance. In the presence of the external confinement the size of the cloud is proportional to the interparticle distance r_0 and is such that characteristic trapping energy is of the same order as the interparticle energy; that is, $V(r_0) \sim \omega_{\text{trap}} r^2$. Taking this into account, one finds that the particle displacement in the mean-field Δ is constant for given trap frequency, $\Delta \sim \alpha(\alpha-1)\omega_{\text{trap}}$, with $\alpha = 3$ for dipoles. The results of the VMC and DMC calculations for radial distribution differ for large values of $d \sim 100$, which means that the gas trial wave function provides an inadequate description of the system in the regime of strong interactions. We repeated our calculation for the trial wave function with shell terms and obtained that radial ordering decreases the energy, but the lowest energy corresponds to both radial and angular localization, i.e., to a crystal phase.

A contour plot of the density profile of particles is shown in Fig. 3. Darker color corresponds to lower density of particles. The internal structure of the shells is not resolved in Fig. 3, as the system can freely rotate due to rotational symmetry. In order to extract information on the shell ordering we introduce the inter- and intra-shell order parameter $\langle \alpha_i \alpha_j \rangle$

with values α_i defined according to

$$\alpha_j = \frac{1}{N_j} \sum_k \exp(i N_j \phi_k), \tag{22}$$

where ϕ_k is the angle of the kth particle in the jth shell containing N_j particles. Each angle ϕ_k is multiplied by a factor of N_j; in this way all contributions are in phase for perfect ordering inside a shell (that is, when $\phi_k = \phi_0 + 2\pi k/L$) and the parameter reaches the maximal value of $\alpha_j = 1$. In

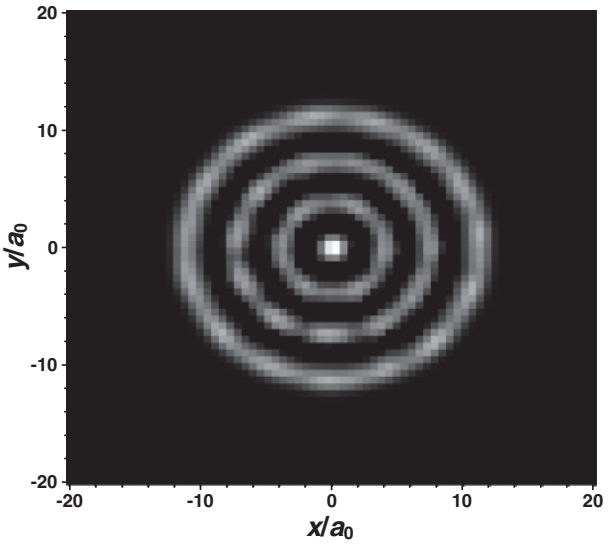

FIG. 3. (x,y) density profile for $N = 32$ particles in the trap for the interaction strength $d = 500$.

the opposite limit of no correlations between particles, this parameter averages to zero. For $i = j$ the function $\langle \alpha_i \alpha_j \rangle$ is the intra-shell order parameter and the larger its value is, the stronger are the internal correlations inside the shell. For $i \neq j$ the function $\langle \alpha_i \alpha_j \rangle$ is the inter-shell order parameter and it measures the correlation strength between shells i and j. The results of DMC simulation for a cluster of $N = 32$ particles with a gas trial wave function (7) are presented in Fig. 4. One finds that the intra-shell order parameter is significantly different from zero for interaction strength larger than $d \sim 100$ and that the inter-shell order parameter is significantly different from zero only for shells 2 and 3 for interaction strength larger than $d \sim 300$. Since we have used the gas trial wave function these correlations are not caused by the symmetry of the trial wave function.

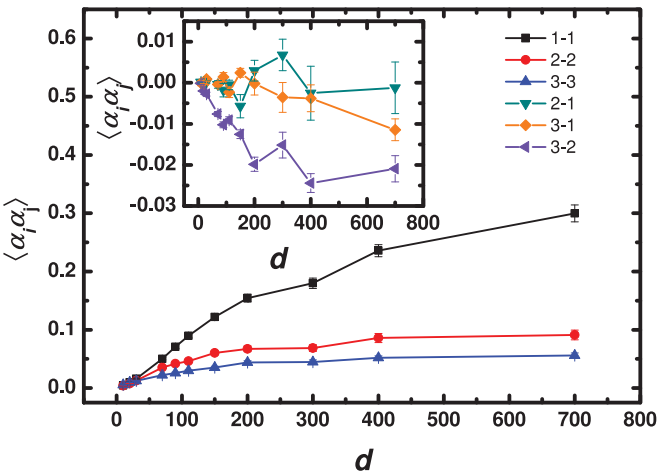

FIG. 4. (Color online) Diagonal (main graph) and nondiagonal (inset) components of the orientational order parameter $\langle \alpha_i \alpha_j \rangle$ with α_i defined as in Eq. (22) for cluster with $N = 32$ particles. Shells are labeled as follows: single particle in the center, first shell, second shell, third shell (see Fig. 3).

To summarize, we suggest the following scenario of $T = 0$ quantum crystallization. When d is small the gas state is energetically favorable; starting from $d \sim 10$ shells are formed in the system, then up to $d \sim 300$ shells solidify and become ordered inside. From $d \sim 200$ shells start to order between each other and around $d \sim 400$ a complete crystal is formed. The central part of a large crystal will show a triangular structure, similar to the one of triangular lattices in untrapped two-dimensional systems [27,28].

B. Bose-Einstein condensation and mesoscopic supersolid

We applied the technique of natural orbitals described in Sec. III, to obtain the fraction of Bose-condensed particles in a cluster of $N = 32$ particles with the interaction strength varying from infinitely small ($d = 0$) to intermediately strong ($d \sim 100$) values.

To test the method used to estimate the condensate fraction we checked that for noninteracting systems all particles are condensed and the condensate wave function coincides with the ground state of the harmonic oscillator. For weak repulsion the density profile monotonically decreases from the maximum in the center of the trap to vanishing density at the borders. Only one orbital is largely occupied and the condensate wave function is monotonous. Strong repulsions create a shell structure in the density profile; see Fig. 5. The condensate wave function is "pushed out" to the border. A similar effect has been found in liquid-helium drops [34] and in trapped gases interacting with hard-core interaction potential [30]. We find that the first few orbitals can be mainly localized in different shells; see Fig. 5. In this situation particles are coherent within a single shell while there is little coherence between different shells.

We find that the condensate is expelled to the regions of low density which is in agreement with slave-boson theory for hard-core gases [35]. This effect can be as well explained within the local density approximation (LDA), that is, by comparing the condensate density $n_0(r) = N_0|\phi_0(r)|^2$ with the condensate occupation $n_0^{\rm hom}[n(r)]$ in a homogeneous system taken for the local density $n(r)$ in the trap. In a homogeneous system the condensate fraction decreases when the density

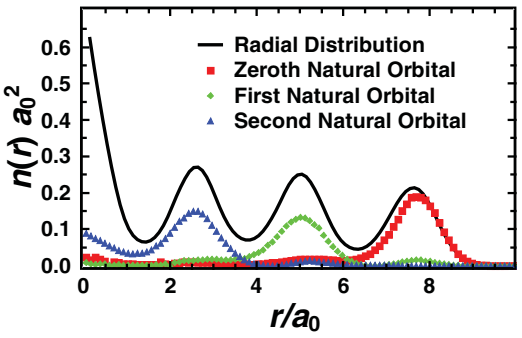

FIG. 5. (Color online) Total density profile $n(r)$ (solid line) compared to densities of the first three orbitals, $n_k(r) = N_k|\phi_k(r)|^2$ (squares, circles, and triangles). The density profile is normalized to the total number of particles N, orbital densities to corresponding eigenvalues $N_k, k = 0,1,2$. All lengths are in units of harmonic oscillator length a_0.

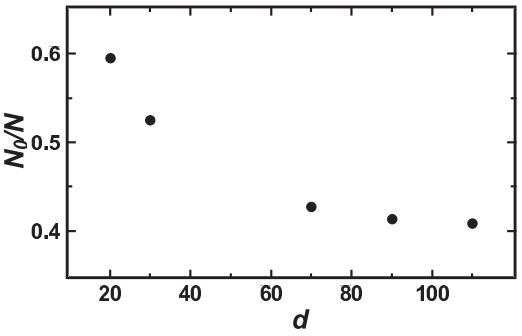

FIG. 6. Fraction of condensed particles N_0/N as a function of the interaction strength d; number of particles in cluster $N = 32$.

is increased. As a result LDA applied to the strong regime results in decrease of the condensate density in the center of the trap. We note, however, that the reasoning based on LDA fails in one-dimensional geometry where lower density means stronger correlations and would wrongly result in condensate density being pushed into the center.

The dependence of the condensate fraction on the interaction strength is presented in Fig. 6. Our calculations show that even in the region of intermediate-strong interactions $d \sim 100$ the fraction of condensed particles significantly differs from zero and is of order 40%. At the same time the shell structure is already formed. The simultaneous coexistence of broken rotational symmetry (shells) and a Bose condensate can be referred to as a mesoscopic supersolid.

V. CONCLUSIONS

In the present work a two-dimensional system of bosonic dipoles in a harmonic trap is studied. Dipoles are assumed to be oriented perpendicularly to the two-dimensional plane and to interact according to repulsive dipole-dipole potential. We found that the cluster undergoes a quantum crystallization for a large value of dipole interaction strength ($d \sim 400$). In the process of zero-temperature transition interaction strength plays the role of a control parameter. We found that crystallization consists of three stages: formation of shells, in-shell ordering, and ordering between shells.

We found that quantum Bose-Einstein condensation occurs in the system. We investigate dependence of the fraction of condensed particles on interaction strength up to the intermediate-strong interaction strengths, and find that the number of particles in the condensate can be sufficiently different from zero. In this regime spatial ordering (shell structure) coexists with Bose condensation, and thus a mesoscopic supersolid is formed.

ACKNOWLEDGMENTS

The work was sponsored by an RFBR grant and the RAS program. G.E.A. acknowledges support by MEC (Spain) and financial support by (Spain) Grant No. FIS2008-04403 and Generalitat de Catalunya Grant No. 2009SGR-1003.

[1] A. Einstein, Sitzber. Kgl. Preuss. Akad. Wiss., 261 (1924).
[2] A. Einstein, Sitzber. Kgl. Preuss. Akad. Wiss., 3 (1925).
[3] F. Dalfovo, S. Giorgini, L. P. Pitaevskii, and S. Stringari, Rev. Mod. Phys. **71**, 463 (1999).
[4] Y. Lozovik and V. Yudson, Sov. Phys. JETP **44**, 389 (1976).
[5] V. B. Timofeev and A. V. Gorbunov, J. Appl. Phys. **101**, 081708 (2007).
[6] A. Griesmaier, J. Werner, S. Hensler, J. Stuhler, and T. Pfau, Phys. Rev. Lett. **94**, 160401 (2005).
[7] J. Stuhler, A. Griesmaier, T. Koch, M. Fattori, T. Pfau, S. Giovanazzi, P. Pedri, and L. Santos, Phys. Rev. Lett. **95**, 150406 (2005).
[8] A. Griesmaier, J. Stuhler, T. Koch, M. Fattori, T. Pfau, and S. Giovanazzi, Phys. Rev. Lett. **97**, 250402 (2006).
[9] T. Lahaye, T. Koch, B. Frohlich, M. Fattori, J. Metz, A. Griesmaier, S. Giovanazzi, and T. Pfau, Nature (London) **448**, 672 (2007).
[10] T. Koch, T. Lahaye, J. Metz, B. Frohlich, A. Griesmaier, and T. Pfau, Nature Phys. **4**, 218 (2008).
[11] S. Ospelkaus, K.-K. Ni, D. Wang, M. H. G. de Miranda, B. Neyenhuis, G. Qumner, P. S. Julienne, J. L. Bohn, D. S. Jin, and J. Ye, Science **327**, 853 (2010).
[12] K.-K. Ni, S. Ospelkaus, D. Wang, G. Quemener, B. Neyenhuis, M. H. G. de Miranda, J. L. Bohn, J. Ye, and D. S. Jin, Nature (London) **464**, 1324 (2010).
[13] M. Saffman, T. G. Walker, and K. Mølmer, Rev. Mod. Phys. **82**, 2313 (2010).
[14] G. Pupillo, A. Micheli, M. Boninsegni, I. Lesanovsky, and P. Zoller, Phys. Rev. Lett. **104**, 223002 (2010).
[15] E. Kim and M. H. W. Chan, Science **305**, 1941 (2004).
[16] E. Kim and M. H. W. Chan, Phys. Rev. Lett. **97**, 115302 (2006).
[17] A. S. C. Rittner and J. D. Reppy, Phys. Rev. Lett. **98**, 175302 (2007).
[18] M. Kondo, S. Takada, Y. Shibayama, and K. Shirahama, J. Low Temp. Phys. **148**, 695 (2007).
[19] A. Penzev, Y. Yasuta, and M. Kubota, J. Low Temp. Phys. **148**, 677 (2007).
[20] Y. Aoki, J. C. Graves, and H. Kojima, Phys. Rev. Lett. **99**, 015301 (2007).
[21] M. C. Keiderling, Y. Aoki, and H. Kojima, J. Phys.: Conf. Ser. **150**, 032040 (2009).
[22] B. Hunt, E. Pratt, V. Gadagkar, M. Yamashita, A. V. Balatsky, and J. C. Davis, Science **324**, 632 (2009).
[23] Y. E. Lozovik and A. I. Belousov, Eur. Phys. J. D **8**, 251 (2000).
[24] Y. E. Lozovik, S. Y. Volkov, and M. Willander, JETP Lett. **79**, 473 (2004).
[25] A. Filinov, J. Böning, M. Bonitz, and Y. Lozovik, Phys. Rev. B **77**, 214527 (2008).
[26] G. E. Astrakharchik, J. Boronat, J. Casulleras, I. L. Kurbakov, and Y. E. Lozovik, in *Recent Progress in Many Body Theories, Proceedings of the Fourteenth International Conference*, edited by J. Boronat, G. E. Astrakharchik, and F. Mazzanti (World Scientific, Singapore, 2008), pp. 245–250.
[27] G. E. Astrakharchik, J. Boronat, I. L. Kurbakov, and Y. E. Lozovik, Phys. Rev. Lett. **98**, 060405 (2007).
[28] H. P. Büchler, E. Demler, M. Lukin, A. Micheli, N. Prokof'ev, G. Pupillo, and P. Zoller, Phys. Rev. Lett. **98**, 060404 (2007).
[29] I. L. Kurbakov, Y. E. Lozovik, G. E. Astrakharchik, and J. Boronat, Phys. Rev. B **82**, 014508 (2010).
[30] J. L. DuBois and H. R. Glyde, Phys. Rev. A **63**, 023602 (2001).
[31] D. S. Lewart, V. R. Pandharipande, and S. C. Pieper, Phys. Rev. B **37**, 4950 (1988).
[32] N. Metropolis, A. W. Rosenbluth, M. N. Rosenbluth, A. H. Teller, and E. Teller, J. Chem. Phys. **21**, 1087 (1953).
[33] G. E. Astrakharchik, A. I. Belousov, and Yu. E. Lozovik, JETP **89**, 696 (1999).
[34] D. S. Lewart, V. R. Pandharipande, and S. C. Pieper, Phys. Rev. B **37**, 4950 (1988).
[35] K. Ziegler and A. Shukla, Phys. Rev. A **56**, 1438 (1997).